# L-curve approach in cross-hole and VSP geophysical diffraction tomography

Eduardo Telmo Fonseca Santos*, IGEO/UFBA and CEFET/BA, Brazil
Amin Bassrei, IF/UFBA and CPGG/UFBA, Brazil

Copyright 2005, SBGf - Sociedade Brasileira de Geofísica

This paper was prepared for presentation at the 9th International Congress of the Brazilian Geophysical Society held in Salvador, Brazil, 11-14 September 2005.

Contents of this paper were reviewed by the Technical Committee of the 9th International Congress of the Brazilian Geophysical Society. Ideas and concepts of the text are authors' responsibility and do not necessarily represent any position of the SBGf, its officers or members. Electronic reproduction or storage of any part of this paper for commercial purposes without the written consent of the Brazilian Geophysical Society is prohibited.

## Abstract

**Since the inverse problem is ill-posed it is necessary to use some tool to reduce this deficiency. The tool that we choose is the regularization by derivative matrices. The L-curve was reintroduced in the literature of inverse problems by Hansen, and, in this work we use the L-curve for the selection of regularization factor in cross hole and VSP geophysical diffraction tomography. Simulations with synthetic data are presented, and the results validate the feasibility of the method.**

## Introduction

The main purpose of exploration geophysics for hydrocarbons is to provide trustworthy images of the subsurface, which could indicate potential hydrocarbons reservoirs. Exploration seismology, better known as seismics is the area of applied geophysics most employed for the subsurface imaging. And within seismics, tomography was incorporated as a method of data inversion. In this work we use geophysical diffraction tomography where the input data is the scattered acoustic field measured at the receivers, and the velocity of the 2-D medium is the inversion output. Since geophysical diffraction tomography is an ill-posed inverse problem, it is necessary to use some tool to reduce this deficiency. The tool that we choose is the regularization of the inverse problem by derivative matrices, known in the literature by several names, specially as Tiknonov regularization. Regularization has an input parameter with crucial role known as regularization parameter or factor, which choice is already a problem. The L-curve was reintroduced in the literature of inverse problems by Hansen (1992a, 1992b, 1998), and, in this work we use the L-curve for the selection of regularization factor in cross hole and vertical seismic profile geophysical diffraction tomography.

## Methodology

Inverse problems have some limitations in such a way that they are said to be ill-posed. Ill-posedness has several causes, and it is present in all geophysical applications. Acoustical tomography, either travel time or diffraction tomography, is not an exception. In this work we study two acquisition geometries in diffraction tomography using the matrix formulation: well to well (cross hole) and well to suface (vertical seismic profiling). The data used is the vector of scattered acoustic field measured at the receivers, and the velocity of the two dimensional medium is the inversion output. One common way to solve this inverse problem is by the generalized inversion through singular value decomposition, where the crucial issue that arises here is the presence of small singular values which generally contribute to inconsistent solutions. This can be avoided, at least partially by using regularization. Instead of using the projection theorem (Devaney, 1984; Wu and Toksöz, 1987), we use the matrix formulation (Rocha Filho et al., 1996; Rocha Filho, 1997; Rocha Filho et al., 1997).. The main advantages of the matrix formulation are: (1) the option of having irregular spacing (i) between sources, (ii) between receivers and (iii) between sources and between receivers (all very common in practical situations with real data); and (2) the possibility to study in a better way the ill-posedness of the inverse problem. The main disadvantage is the cost in terms of computation time. For the forward modeling we compute the scattered acoustic field from a given 2-D velocity distribution $c^{true}(\mathbf{r})$. This is done by using the Born approximation or through a second order finite difference scheme. The scattered field is the input for the inverse procedure, implemented here by singular value decomposition plus regularization. The inversion output is the estimated two-dimensional velocity distribution $c^{est}(\mathbf{r})$. In each inversion we use a different regularization parameter, and we may calculate the RMS error between these two velocities, but our choice of the best regularization parameter is done through the L-curve.

## Generalized Inversion

The concept of generalized inverse was developed by Moore and independently by Penrose (1955). Consider a $M \times N$ matrix $A$. If: (i) $AA^+A = A$; (ii) $A^+AA^+ = A^+$; (iii) $(AA^+)^T = AA^+$; (iv) $(A^+A)^T = A^+A$; then the $N \times M$ matrix $A^+$ is unique and is called pseudo-inverse or generalized inverse. The generalized inverse is calculated using the so-called singular value decomposition (Lanczos, 1961). A rectangular $M \times N$ matrix $A$ with rank $k$ can be decomposed as $A = U\Sigma V^T$ where $U$ is the $M \times M$ matrix which contains the orthonormalized eigenvectors of $AA^T$, $V$ is the $N \times N$ matrix which contains the orthonormalized eigenvectors of $A^TA$ and $\Sigma$ is the $M \times N$ diagonal matrix which contains the

singular values of *A*, written in the decreasing order, that is, $\sigma_1 \geq \sigma_2 \geq \cdots \geq \sigma_k$ .The generalized inverse $A^+$ is a $N \times M$ matrix given by $A^+ = V\Sigma^+ U^T$ where $\Sigma^+$ is the $N \times M$ diagonal matrix which contains the reciprocals of the non-zero singular values of *A*, so that

$$\Sigma^+ = \begin{pmatrix} E & 0 & \cdots & 0 \\ 0 & 0 & \cdots & 0 \\ \vdots & \vdots & \ddots & \vdots \\ 0 & 0 & \cdots & 0 \end{pmatrix}$$

and *E* is the diagonal square matrix of order *k* expressed by

$$E = \begin{pmatrix} \sigma_1^{-1} & 0 & \cdots & 0 \\ 0 & \sigma_2^{-1} & \cdots & 0 \\ \vdots & \vdots & \ddots & \vdots \\ 0 & 0 & \cdots & \sigma_k^{-1} \end{pmatrix}$$

Using SVD the solution will be $\mathbf{m} = A^+\mathbf{d} = V\Sigma^+ U^T\mathbf{d}$.

**Regularization and the L-Curve**

Introducing the concept of regularization (Tikhonov and Arsenin, 1977) in order to improve the quality of the inversion, the solution will be given by $\mathbf{m} = (A^T A + \lambda D^T D)^+ A^T\mathbf{d}$, where $\lambda$ is the regularization factor. If the matrix *D* is equal to the identity the solution reduces to the so called Levenberg-Marquardt expression, or zero order regularization. If *D* is the first derivative matrix then the regularization is called to be first order and so on. The L-curve knee represents a trade-off between smoother solutions with higher errors and rougher solutions with smaller errors. Thus, the knee detection (maximum curvature point) at the L-curve is an heuristic criterium to select the most appropriate solution. Solutions near to the curve knee are also acceptable and possibly more physically meaningful. We applied the L-curve implementing an automatic method to initially select the best regularization factor, but solutions with regularization factor near to the selected one were also considered. Thus, one can achieve a solution that simultaneously satisfy the criteria of error minimization, smoothness and also with physical meaning. Since the problem is ill-posed we use the regularization procedure as did in Gonçalves and Bassrei (1999), but here we employ the L-curve for the selection of the regularization parameter as suggested in Hansen (1992, 1998).

**Diffraction Tomography and Forward Modeling**

The wave equation is given by

$$\nabla^2 U(\mathbf{r},t) = \frac{1}{c^2(\mathbf{r})}\frac{\partial^2 U(\mathbf{r},t)}{\partial t^2},$$

where $U(\mathbf{r},t)$ is the solution (displacement or pressure) and $c(\mathbf{r})$ is the velocity of the medium. Considering that the solution can be written as $U(\mathbf{r},\omega,t) = e^{-i\omega t}P(\mathbf{r},\omega)$, which represents a harmonic dependence with time, we obtain the Helmholtz equation: $[\nabla^2 + k^2]P(\mathbf{r},\omega) = 0$, where the 2-D wavenumber is given by $k = k(\mathbf{r},\omega) = \sqrt{k_x^2 + k_y^2}$. The conditions for the imaging are that the medium is acoustic and 2-D, and the propagation of the incident field is within an limited area $A(\mathbf{r}')$, the background, with constant velocity $c_0$. The object function is defined as

$$O(\mathbf{r}) = 1 - \frac{c_0^2}{c^2(\mathbf{r})},$$

and represents the perturbation of the velocity in each point in relation to $c_0$. Redefining the wavenumber as function of $O(\mathbf{r})$, we have that $k^2(r) = k_0^2 - k_0^2 O(\mathbf{r})$, and substituting it in the Helmholtz equation, we obtain

$$[\nabla^2 + k^2]P_{SCAT} = k_0^2 O(\mathbf{r})[P_0 + P_{SCAT}],$$

where $P_0$ is the incident field and $P_{SCAT}$ is the scattered field. The last differential equation has the following integral solution, known as Lippmann-Schwinger equation(Lo and Inderwiesen, 1994):

$$P_{SCAT}(\mathbf{r}) = -k_0^2 \int_{A(\mathbf{r}')} O(\mathbf{r}')G(\mathbf{r} \mid \mathbf{r}')[P_0(\mathbf{r}') + P_{SCAT}(\mathbf{r}')]d\mathbf{r}'.$$

In the inverse scattering procedure, we consider the knowledge of the scattered field, so that the object function is the unknown function, and the integral solution becomes an integral equation. The above equation is nonlinear and the linearization is achieved, for example, via the first order Born approximation, which is only valid for the weak scattering of the incident field. The total field is $P_T(\mathbf{r}) = P_0(\mathbf{r}) + P_{SCAT}(\mathbf{r})$ so that we have $P_T(\mathbf{r}) = P_0(\mathbf{r})$. Thus we obtain a linear relation between $O(\mathbf{r})$ and $P_S(\mathbf{r})$ : $P_{SCAT}(\mathbf{r}) = -k_0^2 \int_{A(\mathbf{r}')} O(\mathbf{r}')G(\mathbf{r} \mid \mathbf{r}')P_0(\mathbf{r}')d\mathbf{r}'.$

We represent the incident field by a source in $\mathbf{r}_S$ through the Green's function: $P_0(\mathbf{r}') = G(\mathbf{r}' \mid \mathbf{r}_S)$, and the scattered field in $A(\mathbf{r})$ is registered by a receptor in $\mathbf{r}_G$ :

$$P_{SCAT}(\mathbf{r}_S, \mathbf{r}_G) = -k_0^2 \int_{A(\mathbf{r}')} O(\mathbf{r}')G(\mathbf{r}' \mid \mathbf{r}_S)G(\mathbf{r}_G \mid \mathbf{r}')d\mathbf{r}'$$

The discretization of the above relation leads to the linear relation **d** = *A***m**, which has to be inverted in order to recover *O*(r). In this work the inversion is done using SVD.

The scattered field computed from the synthetic model was performed using finite differences, assuming a Ricker's wavelet source signature. However, the calculated field at the source position has differences of amplitude and phase in relation to the original Ricker's wavelet. The calculated field amplitude is $2\pi$ times greater than the adopted wavelet's amplitude and there is a constant phase shift depending on the selected frequency. Calibration was performed to correct these differences by the average complex ratio between Born approximation and finite difference modeling. Another possible calibration consists of filter calculation that

transforms the measured field into the corresponding Ricker's wavelet and then this filter is applied to the synthetic seismograms.

**Numerical Simulation**

We considered a true model with 15 x 15 = 225 blocks, which can be seen in Figure 1 for the cross well geometry and in Figure 9 for the VSP geometry. The same true models can be seen in Figure 2 and Figure 10 with a different display. The background medium has 4,000 *m/s*. There is a low velocity layer with 3,900 *m/s*. This makes a minus 2.5 % contrast. The central inhomogeneity has 4,100 *m/s* which is equivalent to a plus 2.5 % anomaly. In each configuration there are 16 sources and 16 receivers, in such a way that the data set has 256 complex numbers. Figures 1, 2, 9 and 10 also show the source and receiver location. But since we separate the complex numbers in real and imaginary parts, we have in fact 512 informations, making the tomographic matrix rectangular (512 x 225). The frequency of the monochromatic wave is 210 *Hz*. All the following simulations are with noisy data. Basically we add Gaussian noise in such a level that the RMS between the original scattered field and the corrupted one is around 1%. For each example we produced three L-curves: for the regularizations of zero, first and second order. The Hansen's package provides the "corner" of the L-curve. In the caption of each tomogram we provide information of this "optimal" regularization parameter and the RMS error between the true velocity and the estimated one, and also the RMS error between the true object function and the estimated one. Figure 3 shows the L-curve for zero order and Figure 4 shows the reconstruction. For the first order the L-curve can be seen in Figure 5 and the reconstruction in Figure 6. For the second order the L-curve is displayed in Figure 7 and estimated model in Figure 8. For the VSP geometry, Figure 11 shows the L-curve for zero order and Figure 12 shows the reconstruction. For the first order the L-curve can be seen in Figure 13 and the reconstruction in Figure 14. For the second order the L-curve is displayed in Figure 15 and estimated model in Figure 16. For comparison, the reconstructions with least squares, that is without regularization can be seen in Figures 17 and 18.

**Conclusions**

From two sets of overdetermined synthetic examples with ill-conditioned kernel matrix we have shown that the algorithm in question is feasible for a regularization algorithm for geophysical diffraction tomography. It performed well when compared with other inversion techniques such as non-regularized SVD. In relation to the regularization factor selection, we used the L-curve in order to make a decision about the optimal parameter.

**Acknowledgements**

This work is part of the project *Multi-Dimensional and Spectral Seismic Processing in High Resolution Seismo-stratigraphy,* sponsored by the edict *CTPETRO/CNPq-FINEP 03/2001*. The authors also thank the support from *PETROBRAS*. One author (AB) also thanks the support from *PGS Brazil*.

**References**

**Devaney, A. J**., 1984, Geophysical diffraction tomography. IEEE Transactions on Geoscience and Remote Sensing, 22, 3-13.

**Gonçalves, M. R. G, e Bassrei, A.**, 1999, Um experimento numérico em tomografia geofísica de difração, 6º Congresso Internacional da Sociedade Brasileira de Geofísica, Rio de Janeiro, RJ, Brasil, CDROM, resumo SBGF254.

**Hansen, P. C.**, 1992a, Analysis of discrete ill-posed problems by means of the l-curve, SIAM Review, 34, 561-580.

**Hansen, P. C.**, 1992b, Regularization Tools. A Matlab Package for Analysis and Solution of Discrete Ill-Posed Problems, Technical University of Denmark, Lyngby, Denmark.

**Hansen, P. C.,** 1998, Rank-Deficient and Discrete Ill-Posed Problems. SIAM, Philadelphia.

**Lanczos, C.**, 1961, Linear Differential Operators. Van Nostrand, London.

**Lo, T.-w., and Inderwiesen, P. L.**, 1994, Fundamentals of Seismic Tomography. Geophysical Monograph Series. SEG, Tulsa (OK).

**Penrose, R.**, 1955, A generalized inverse for matrices. Proceedings of the Cambridge Philosophical Society, 51, 406-413

**Rocha Filho, A. A., Harris, J. M., and Bassrei, A.**, 1996, A simple matrix formulation diffraction tomography algorithm, XXXIX Congresso Brasileiro de Geologia, Salvador, BA, Brasil, volume 2, p. 312-315.

**Rocha Filho, A. A.**, 1997, Formulação Matricial Multifreqüência e Inversão Integrada, Dissertação de Mestrado, UFBA.

**Rocha Filho, A. A., Harris, J. M., e Bassrei, A.**, 1997, Inversão integrada de dados sísmicos utilizando tomografia de difração, 5º Congresso Internacional da Sociedade Brasileira de Geofísica, São Paulo, SP, Brasil, volume II, p. 630-634.

**Tikhonov, A. N., and Arsenin, V. Y.**, 1977, Solution of Ill-Posed Problems, Wiley, Washington, D.C.

**Wu, R-S, and Toksöz, M. N**., 1987, Diffraction tomography and multisource holography applied to seismic imaging. Geophysics, 52, 11-25.

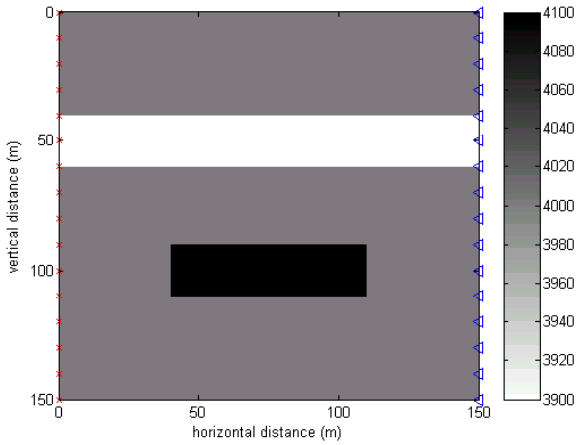


Figure 1. True model
(Cross well acquisition geometry - XWP)

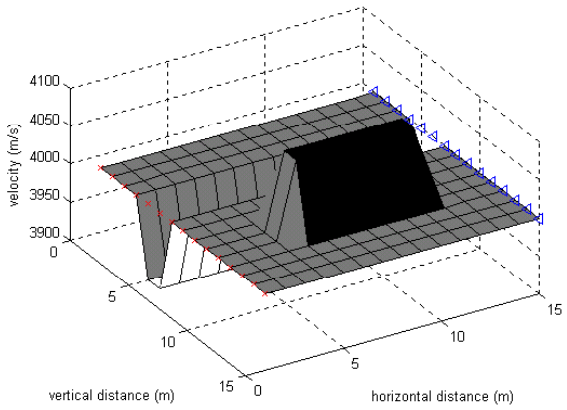


Figure 2. True model 15×15 mesh (XWP)

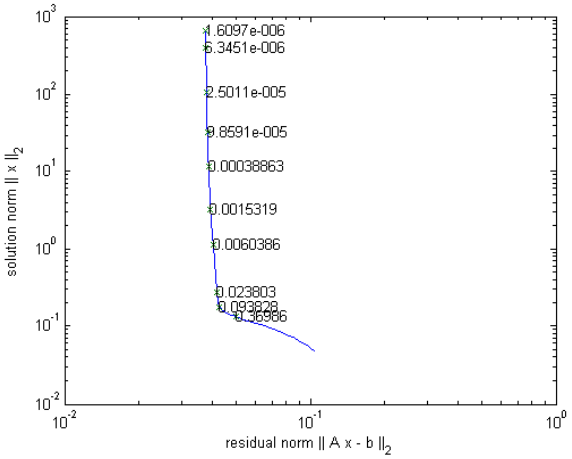


Figure 3. L-curve for zero order regularization (XWP)

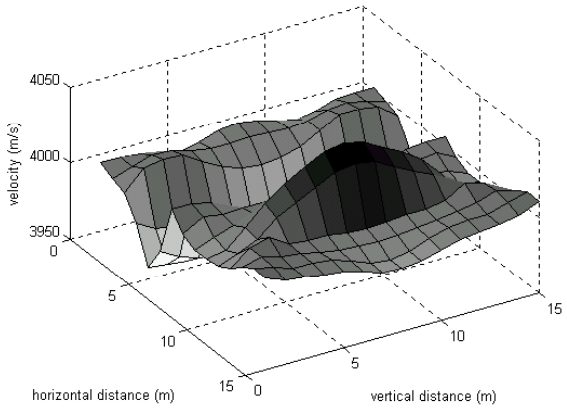


Figure 4. Tikhonov inversion (zero order regularization)
$\lambda$=0.30108; $RMS_c$=0.50287%; $RMS_o$=24.6535%

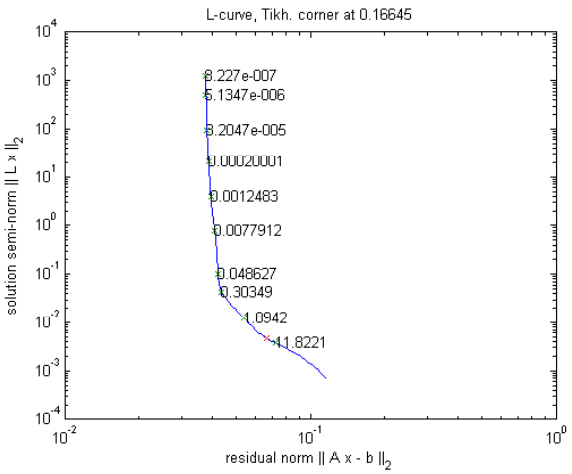


Figure 5. L-curve for first order regularization (XWP)

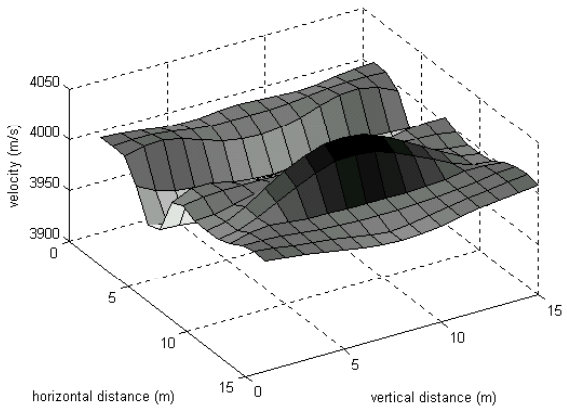


Figure 6. Tikhonov inversion (first order regularization)
$\lambda$=0.5761; $RMS_c$=0.48179%; $RMS_o$=22.3163%

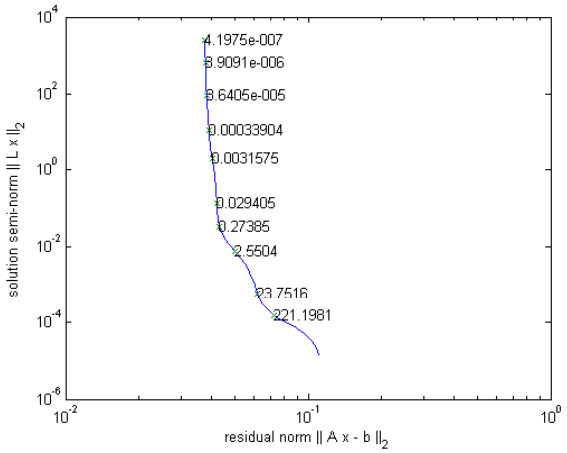


Figure 7. L-curve for second order regularization (XWP)

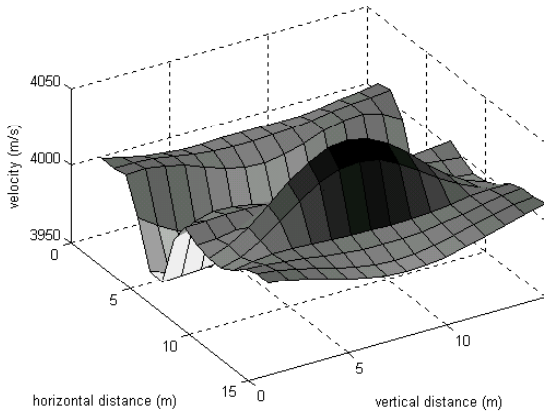


Figure 8. Tikhonov inversion (second order regularization)
$\lambda$=1.4599; $RMS_c$=0.48227%; $RMS_o$=25.9723%

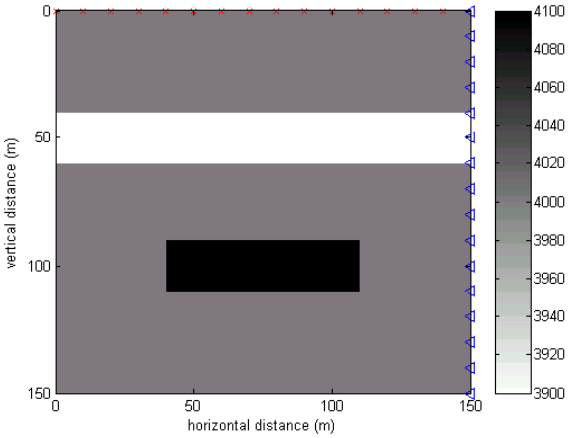


Figure 9. True model
(Vertical Seismic Profile – VSP)

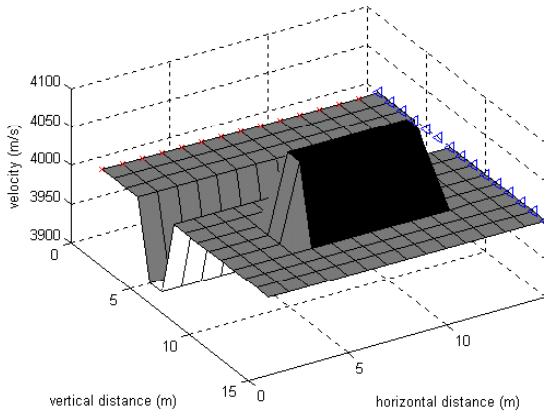


Figure 10. True model 15×15 mesh (VSP)

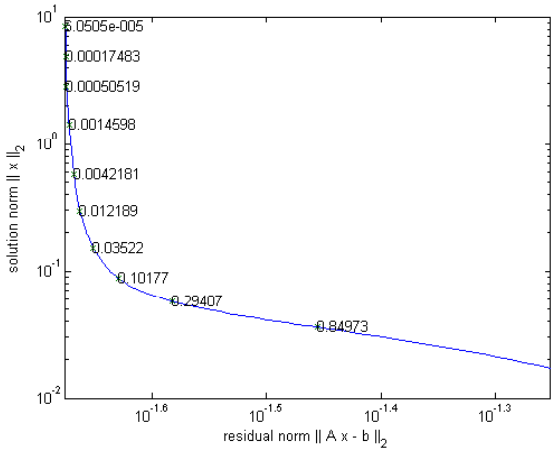


Figure 11. L-curve for zero order regularization (VSP)

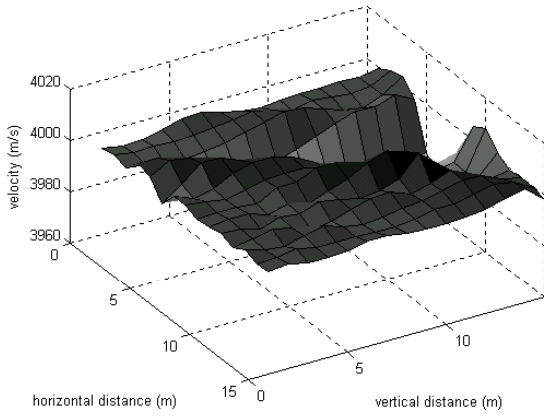


Figure 12. Tikhonov inversion (zero order regularization)
$\lambda$=0.32699; $RMS_c$=0.59085%; $RMS_o$=40.0224%

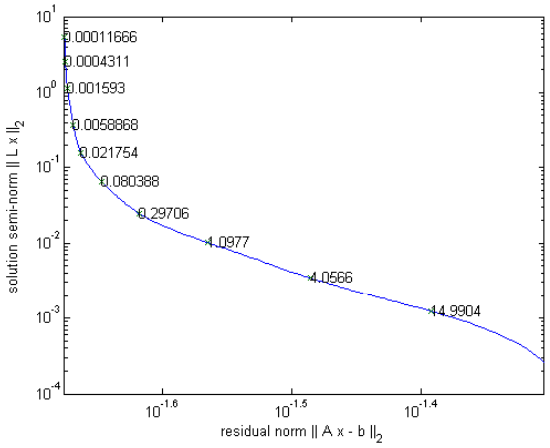


Figure 13. L-curve for first order regularization (VSP)

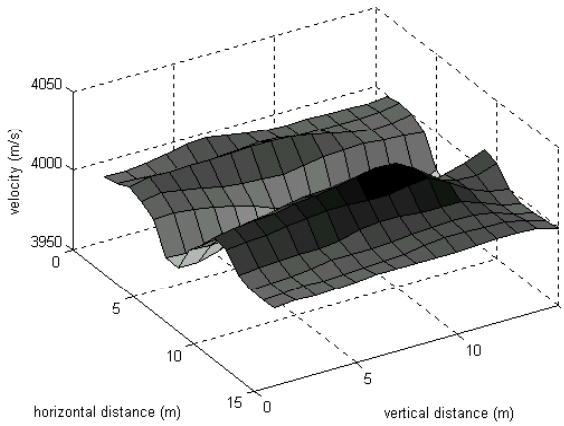


Figure 14. Tikhonov inversion (first order regularization)
$\lambda$=0.50108; $RMS_c$=0.53196%; $RMS_o$=81.7048%

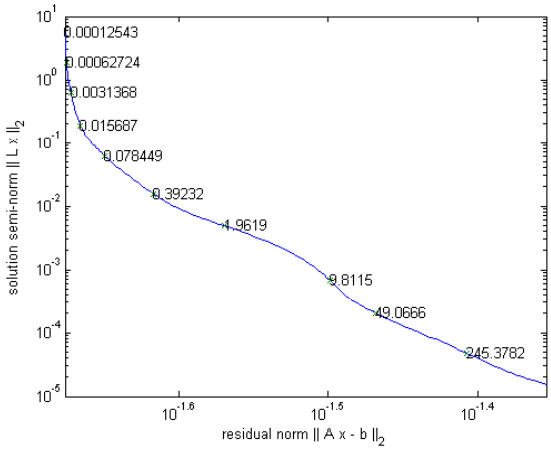


Figure 15. L-curve for second order regularization (VSP)

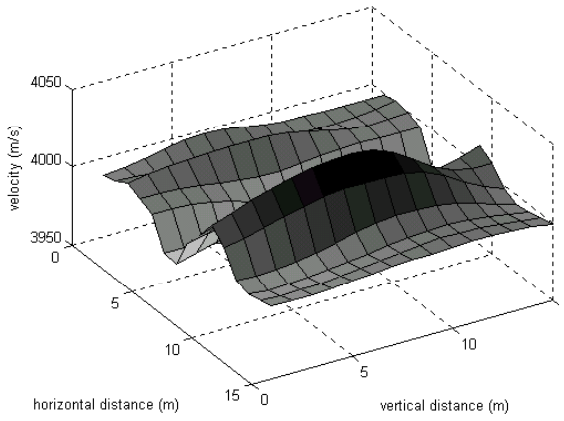


Figure 16. Tikhonov inversion (second order regularization)
$\lambda$=1.0305; $RMS_c$=0.5253%; $RMS_o$=85.7834%

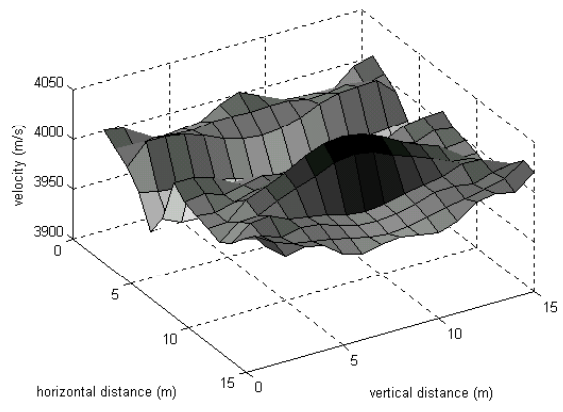


Figure 17. Least squares solution for XWP acquisition
$RMS_c$=0.52655%; $RMS_o$=65.5594%

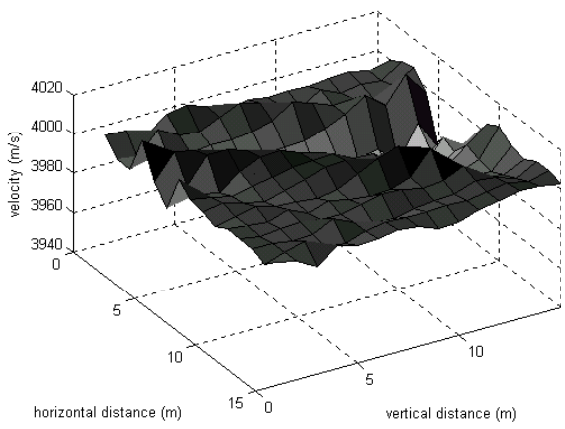


Figure 18. Least squares solution for VSP acquisition
$RMS_c$=0.61016%; $RMS_o$=92.1246%